

## Phase relations and dehydration behaviour of calcareous sediments at very-low to low grade metamorphic conditions

Hans-Joachim Massonne \*

institut für mineralogie und Kristallchemie, Universität stuttgart, azenbergstr. 18, D-70174 stuttgart, Germany

**Abstract** - P-t pseudosections were calculated in the system  $\text{SiO}_2\text{-TiO}_2\text{-Al}_2\text{O}_3\text{-MgO-MnO-FeO-O}_2\text{-CaO-Na}_2\text{O-K}_2\text{O-H}_2\text{O-CO}_2$  with the **PerPLEx** software package for the pressure-temperature range 1-25 kbar and 150-450°C to gain a better understanding of the phase relations of metamorphosed calcareous sediments at low temperature including their dehydration behaviour during prograde metamorphism. For this purpose the applied thermodynamic data set of Holland and Powell, augmented by data of massonne and Willner, was enlarged by end-member data for **mn-stilpnomelane**. In addition, a three-component solid-solution model for **stilpnomelane** and a four-component model for **Ca-Mg-Mn-Fe carbonate** with calcite structure were introduced.

For geotherms of 10-15°C/km, which are typical for the metamorphism of rocks involved in accretionary wedge systems, a major dehydration event occurs at temperatures between 270 to 330°C in both carbonate-free and calcareous greywackes. For an investigated marly limestone this event takes place at about 100°C higher temperatures. The **H<sub>2</sub>O-CO<sub>2</sub>** fluid formed is characterized by very low **CO<sub>2</sub>** contents. The major dehydration event is made responsible for the detachment of sediments on top of a subducting slab.

**Riassunto** - al fine di migliorare le conoscenze sulle

relazioni di fase a bassa temperatura in metasedimenti a diverso contenuto in carbonati e sulla loro disidratazione durante il metamorfismo progrado, sono state calcolate differenti pseudosezioni P-t nel sistema  $\text{SiO}_2\text{-TiO}_2\text{-Al}_2\text{O}_3\text{-MgO-MnO-FeO-O}_2\text{-CaO-Na}_2\text{O-K}_2\text{O-H}_2\text{O-CO}_2$ , utilizzando il software **PerPLEx** nell'intervallo 1<P<25 kbar e 150<t<450°C. Per rendere possibile una modellizzazione più completa, nuovi parametri termodinamici per il termine **mn-stilpnomelano** e recenti dati di massonne e Willner sono stati inseriti nel database termodinamico di Holland & Powell. I modelli relativi alle soluzioni solide disponibili in letteratura sono stati integrati da un modello a tre componenti per lo **stilpnomelano** e da un modello quaternario **Ca-Mg-Mn-Fe** per il carbonato con struttura della calcite. assumendo geoterme di 10-15°C/Km (condizioni tipiche per il metamorfismo di rocce coinvolte nei cunei di accrezione), la maggior parte della disidratazione avviene a temperature comprese tra 270 e 330°C per composizioni corrispondenti a grovacke, sia povere che ricche in carbonati. nel caso di calcari marnosi, la disidratazione ha luogo a temperature più alte di circa 100°C. La composizione del fluido, nel sistema modello **H<sub>2</sub>O-CO<sub>2</sub>**, risulta caratterizzata da un contenuto molto basso di **CO<sub>2</sub>**. Questo importante evento di disidratazione può essere considerato responsabile del distacco dei sedimenti situati nella parte superiore dello slab in subduzione.

**Key words:** *calcareous metasediment; subduction zone; accretion; dehydration; decarbonation; thermodynamic calculations of phase relations.*

### introduction

The understanding of phase relations at very-low to low grades of metamorphism has been gradually improved over the last decades first by the development of petrogenetic grids deduced from observations on natural rocks (e.g. Brown, 1975; Liou *et al.*, 1985, 1987) and subsequently by the consideration of thermodynamic relations and data for rock-forming minerals for the construction of such grids (e.g. Evans, 1990; Frey *et al.*, 1991; Thye *et al.*, 1992). Recently, Massonne and Willner (2008) presented thermodynamic data for stilpnomelane and pumpellyite solid solutions to better consider phase relations for the P-t range of very-low grade metamorphism. These authors applied a method of Gibbs energy minimization for a specific rock composition to calculate phase relations within a given P-t frame (so-called P-t pseudosection). The computer program package *PerPLe\_X* (see Connolly, 2005) allowed them additionally to calculate the content of water in solids in the P-t frame of 1-25 kbar and 150-450°C and, thus, to quantify the dehydration behaviour of various rocks at very-low to low grade metamorphic conditions. From the results on mid-ocean ridge basalts and a psammopelitic rock typical for sediments deposited at active continental margins, Massonne and Willner (2008) concluded that a significant dehydration event occurs in such clastic sediments on top of an oceanic crust during early subduction. Corresponding P-t conditions are, for instance, about 5 kbar and 240°C or 8 kbar and 280°C. This dehydration event was assumed to be the cause of the initiation of accretion of clastic sediments whereas the oceanic crust below these sediments, dehydrating at higher temperatures, is

contemporaneously more deeply subducted. Thus, an accretionary wedge forming by this process should consist mainly of clastic sediments. A good natural example might be the Late Palaeozoic to Mesozoic accretionary wedge system which is now exposed along the coast of central to southern Chile (Massonne and Willner, 2008). The metasediments of this fossil accretionary wedge system are more or less carbonate-free and, thus, are compatible with the psammopelite selected for the study by Massonne and Willner (2008). However, other fossil accretionary wedge systems, for instance in the circum-Pacific region, can contain considerable quantities of carbonate in the metasediments. This concerns, for instance, greywackes of the Franciscan formation, California, and in particular metasediments of the Sanbagawa belt, Japan (Goto *et al.*, 2007). In order to test whether the aforementioned conclusion by Massonne and Willner (2008) could be also valid for carbonate-bearing metasediments, further rock compositions are studied here using the *PerPLe\_X* software package in order to compare their dehydration behaviour with that of the psammopelite investigated by these authors. For this purpose, two rock compositions were selected representing somewhat distinct calcareous greywackes. A third rock composition for this comparison study is a marly sediment with significant amounts of calcite/aragonite.

### Rock compositions and calculation method

The P-t pseudosections were calculated for compositions of an Eocene greywacke (Pettijohn, 1949) from Washington state, USA, and the global subducted sediment (Gloss), which is an average composition estimated by Plank and Langmuir (1998). Both rocks contain about 7% carbonate but they differ, for instance, in regard to the contents of SiO<sub>2</sub>, Al<sub>2</sub>O<sub>3</sub>, and Na<sub>2</sub>O, which are higher in the Eocene greywacke

(see table 1). the GLOSS composition was also used by Kerrick and Connolly (2001) to calculate the devolatilization of subducted sediments using the same method as applied in this study. However, the investigation of these authors is related to higher temperatures than those considered here. In addition to the two sediments containing moderate contents of carbonate, a rock significantly richer in carbonate was taken into account. The metamorphosed marly limestone is from Crete (Theye, 1988; sample no. K84/433) and might represent an average for the originally <1000 m thick package of intensively layered limestones, shales and other kinds of sedimentary rocks of the Permian Phyllite-Quartzite (PQ) unit. The original compositions were simplified

(table 1) to fit the twelve-component system  $SiO_2$ - $TiO_2$ - $Al_2O_3$ - $MgO$ - $MnO$ - $FeO$ - $O_2$ - $CaO$ - $Na_2O$ - $K_2O$ - $H_2O$ - $CO_2$ . An oxygen content was chosen for the calcareous greywacke that relates to about 10%  $Fe^{3+}$  of the total iron, as previously done by Massonne *et al.* (2007) and Massonne and Willner (2008). However, for GLOSS a higher  $O_2$  content, corresponding to about 25%  $Fe^{3+}$  of the total iron, was selected in order to test the possible influence of more highly oxidised rocks on the evolution of mineral assemblages and dehydration. For the marly limestone an even higher  $O_2$  content was chosen because the PQ unit in Crete can contain highly oxidised rocks as discernable by abundant hematite in the low-grade metamorphic rocks of this unit. The high water content of 7.3 wt.% in GLOSS is that

**Table 1**  
Rock compositions (A = original, B = normalized) used for the calculation of P-T pseudosections. The composition of the metapsammopelite was taken from Massonne and Willner (2008) for comparison.

	metapsammo -pelite	calcareous Greywacke		GLOSS		marly Limestone	
(wt.%)	b	a	b	a	b	a	b
SiO <sub>2</sub>	60.75	65.05	62.91	58.57	58.75	28.40	27.77
TiO <sub>2</sub>	0.70	0.46	0.44	0.62	0.62	0.43	0.42
Al <sub>2</sub> O <sub>3</sub>	17.77	13.89	13.43	11.91	11.95	10.30	10.07
Feo	5.60	*3.266	3.16	5.21	5.23	*3.07	3.00
O <sub>2</sub>	0.06	*0.074	0.04	**0.15	0.15	*0.27	0.20
MnO	-	0.11	0.11	0.32	0.32	0.05	0.05
MgO	2.48	1.22	1.18	2.48	2.49	1.50	1.47
CaO	0.84	5.62	5.25	5.95	***5.72	29.20	28.69
Na <sub>2</sub> O	2.55	3.13	3.03	2.43	2.44	0.25	0.24
K <sub>2</sub> O	3.25	1.41	1.36	2.04	2.05	0.64	0.63
H <sub>2</sub> O	6.00	2.58	5.50	7.29	7.30	3.80	6.00
CO <sub>2</sub>	-	2.83	3.50	3.01	3.00	22.20	21.80
sum	100.00	99.64	100.00	99.98	100.00	100.11	100.00

For data sources see text. all analyses were normalized to 100 wt.% after adding some wt.% of CO<sub>2</sub>, compatible with a reasonable amount of calcite in the rock at near-surface conditions, and H<sub>2</sub>O to the rock to ensure an H<sub>2</sub>O-rich fluid in excess for (at least a wide range of) the P-T conditions of the pseudosections. \* in the originally quoted analysis, contents of Feo and Fe<sub>2</sub>O<sub>3</sub> were given instead of Feo and O<sub>2</sub>; \*\* assumed value; \*\*\* the value of CaO was reduced corresponding to a P<sub>2</sub>O<sub>5</sub> content of 0.19 wt.% in the original analysis as this content was related to pure apatite Ca<sub>5</sub>(PO<sub>4</sub>)<sub>3</sub>(F,Cl,OH).

reported by Plank and Langmuir (1998). The water contents in the other two rock compositions (Table 1) were thus selected that some free water appeared in the calculation results already at (greywacke) or almost at (marly limestone) the lowest P-T conditions of 1 kbar and 150°C.

The P-T pseudosections were calculated with the *PerPLe\_X* version from August 2006, downloaded from the internet site <http://www.perplex.ethz.ch/>, for the P-T frame of 1-25 kbar and 150-450°C. as reported by Massonne and Willner (2008), the thermodynamic data set of Holland and Powell (1998, updated 2002) for minerals and H<sub>2</sub>O-CO<sub>2</sub> fluid (model *corK*) was used, including solid-solution models (see, e.g. Powell and Holland, 1999) compatible with this data set. Thus, the subsequent models were chosen from the downloaded version of the *PerPLe\_X* solution model file (*newest\_format\_solut.dat*): *bio*(HP) for biotite (annite - phlogopite - mn-biotite + components considering tschermak's substitution such as eastonite), *chl*(HP) for chlorite (clinochlore-amesite and corresponding Fe<sup>2+</sup>-mn-bearing components), *ctd*(HP) for Fe<sup>2+</sup>-mg-mn chloritoid, *ep*(HP) for clinozoisite-epidote, *Gt*(HP) for garnet (almandine-grossular-pyropespartine, the maximum content of spessartine was limited to 50 mol%), *Pheng*(HP) for potassic white mica (muscovite - paragonite - mg-al celadonite - Fe<sup>2+</sup>-al celadonite, the maximum content of paragonite was limited to 20 mol%). For feldspars the model by Fuhrman and Lindsley (1988) was applied, but it was subdivided for practical reasons into separate models for plagioclase (*fsp1*) and alkali-feldspar (*fsp2*) by limiting the compositional range to a maximum of 10 mol% K-feldspar component (*fsp1*) or 5 mol% anorthite + 75 mol% albite component (*fsp2*). Also applied were the solid-solution models for pumpellyite [*Pu*(m): mg-pumpellyite - Fe<sup>2+</sup>-pumpellyite - Fe<sup>2+</sup>Fe<sup>3+</sup>-pumpellyite = Ca<sub>4</sub>Al<sub>4</sub>Fe<sup>3+</sup>Fe<sup>2+</sup>Si<sub>6</sub>O<sub>21</sub>(OH)<sub>7</sub>], low-

temperature amphibole [*act*(m): tremolite - glaucophane - mg-riebeckite - actinolite = Ca<sub>2</sub>Mg<sub>3</sub>Fe<sup>2+</sup><sub>2</sub>Si<sub>8</sub>O<sub>22</sub>(OH)<sub>2</sub>], and na-clinopyroxene with space group *c2/c* [*acm*(m): aegirine (formerly acmite) - jadeite - diopside - hedenbergite], as newly introduced by Massonne and Willner (2008). Models for further solid solutions are reported in the subsequent section. Phases *h2oL* (H<sub>2</sub>O in silicate melt), *vsv* (vesuvianite), *andr* (andradite), *tpz* (OH-topaz), *rieb* (riebeckite), *ab* (low-albite), and *mic* (microcline) in the applied data file were excluded. In addition to the P-T pseudosections contoured P-T graphs were also produced containing, for instance, isopleths for the content of Si in phengite. The graphical results produced with sub-programs of *PerPLe\_X* (*vertex*, *psvdraw*, *werami*, and *pscontor*) were redrawn by smoothing curves, as demonstrated by Connolly (2005), to obtain the final pseudosections (Figs. 1, 2, and 4) and contoured P-T diagrams (Figs. 1 and 3-5). Information on a mineral assemblage at specific P-T conditions, such as the composition of a specific solid-solution phase, could be taken from printable files generated by the sub-program *vertex*. In reconnaissance runs the compositional ranges of the considered solid-solution phases were explored so that for a final run their compositional ranges could be correspondingly reduced and their resolutions enhanced approaching the maximum number of one million pseudo-component compounds. By this procedure, the quality of the graphical results before smoothing was optimized.

imProveD soLID-soLUTION moDeLs For siLicates  
anD carbonates

in the study by Massonne and Willner (2008) a few phases such as albite were assumed to occur with end-member composition although these phases can show considerable solid-solution towards specific end-members.

However, at low temperatures ( $\leq 450^\circ\text{C}$ ) such solid solutions are often limited, justifying such simplifications made by these authors. nevertheless, in this study it was attempted to consider also minor solid-solutions. in addition, the introduction of mno into the system, compared with the system of the previous study by massonne and Willner (2008), required the consideration of possible mn-bearing end-member phases. Furthermore, a new group of minerals, carbonates, appears due to the introduction of  $\text{CO}_2$  in the chemical system. For these minerals, appropriate solid-solution models had to be tested and eventually further developed.

#### Silicates

the available solid-solution models for paragonite (2) in file newest\_format\_solut.dat consider only binary solid-solutions, namely towards muscovite (1) or margarite (3). thus, a ternary model was created for paragonite adopting the margules parameters for the muscovite-paragonite join from chatterjee and Froese (1975):  $W_{122} = 19456 \text{ J/mol} - \mathbf{t} \cdot 1.6544 \text{ J/(mol}\cdot\text{K)} + \mathbf{P} \cdot 0.4561 \text{ J/(mol}\cdot\text{bar)}$ ,  $W_{112} = 12230 \text{ J/mol} - \mathbf{t} \cdot 0.71044 \text{ J/(mol}\cdot\text{K)} + \mathbf{P} \cdot 0.6653 \text{ J/(mol}\cdot\text{bar)}$  with  $\mathbf{t}$  and  $\mathbf{P}$  in K and bar, respectively. margules parameters for the paragonite-margarite series were derived on the basis of an asymmetric solvus (see Franz *et al.*, 1977) leading to  $W_{233} = 18.2 \text{ kJ/mol}$  and  $W_{223} = 10 \text{ kJ/mol}$ . For the muscovite-margarite series, which shows an extended solvus range similar to the K-feldspar-anorthite series, a correspondingly high margules parameter  $W_{133} = W_{113} = 35 \text{ kJ/mol}$  was selected. no ternary parameter was introduced. this new solid-solution model was subdivided for practical reasons into two models [Pa(m) and mama(m)] limiting the maximum content of the three mica components differently. For instance, for the composition of the marly limestone, the following limits were applied: (a) for paragonite [model Pa(m)] 35 mol%

margarite and 25 mol% muscovite component, (b) for margarite [model mama(m)] 20 mol% paragonite and 0 mol% muscovite component.

the binary  $\text{Fe}^{2+}$ -mg-stilpnomelane model by massonne and Willner (2008) was enlarged by the corresponding  $\text{mn}^{2+}$  end-member  $\text{K}_{5.5}\text{al}_{5.5}\text{mn}^{2+}_{48}\text{si}_{67}\text{O}_{168}(\text{OH})_{48} \cdot 36 \text{ H}_2\text{O}$ . in fact, the solid solution among all three end-members was assumed to be ideal but reasonable thermodynamic properties for the  $\text{mn}^{2+}$  end-member had to be derived. For this purpose, the parameters for the  $c_p$  function ( $= k_0 + k_1 \cdot \mathbf{t}^{0.5} + k_2 \cdot \mathbf{t}^2 + k_3 \cdot \mathbf{t}^3$  with  $k_0 = 12238.78$ ,  $k_1 = -96778.0$ ,  $k_2 = -181141800$ ,  $k_3 = 28334130000$ ; units in J

and K) and the molar entropy (7642 J/(mol K)) at standard state was estimated according to berman and brown (1985) and Holland (1989), respectively. the estimation of the molar volume of the theoretical  $\text{mn}^{2+}$ -stilpnomelane end-member (313.3 J/(mol · bar)) at standard state was accomplished by the consideration of the volume difference between end members of various  $\text{Fe}^{2+}$ - $\text{mn}^{2+}$ -silicate solid-solution series given in the data set by Holland and Powell (1998). For expansivity and compressibility the assumption was made that  $\text{mn}^{2+}$ -stilpnomelane shows the same characteristics as  $\text{Fe}^{2+}$ -stilpnomelane (see massonne and Willner, 2008). only the enthalpy of formation (or here Gibbs energy of formation) of  $\text{mn}^{2+}$ -stilpnomelane had to be determined. For the derivation of  $\Delta G_f$  at standard state of this end member the distribution of  $\text{mn}^{2+}$  and  $\text{Fe}^{2+}$  among the pair (mn-rich) garnet - stilpnomelane was considered. this assemblage occurs at low temperatures (300-400°C) and high pressures (>8 kbar) as pointed out by massonne and szpurka (1997). Literature data, taken, for instance, from robinson (1984) and Piber *et al.* (2009), as well as own electron-microprobe measurements on low-grade metamorphic rocks from the Franciscan formation, california, and the antarctic Peninsula (elephant island) allow us to determine the distribution of  $\text{mn}^{2+}$  and  $\text{Fe}^{2+}$



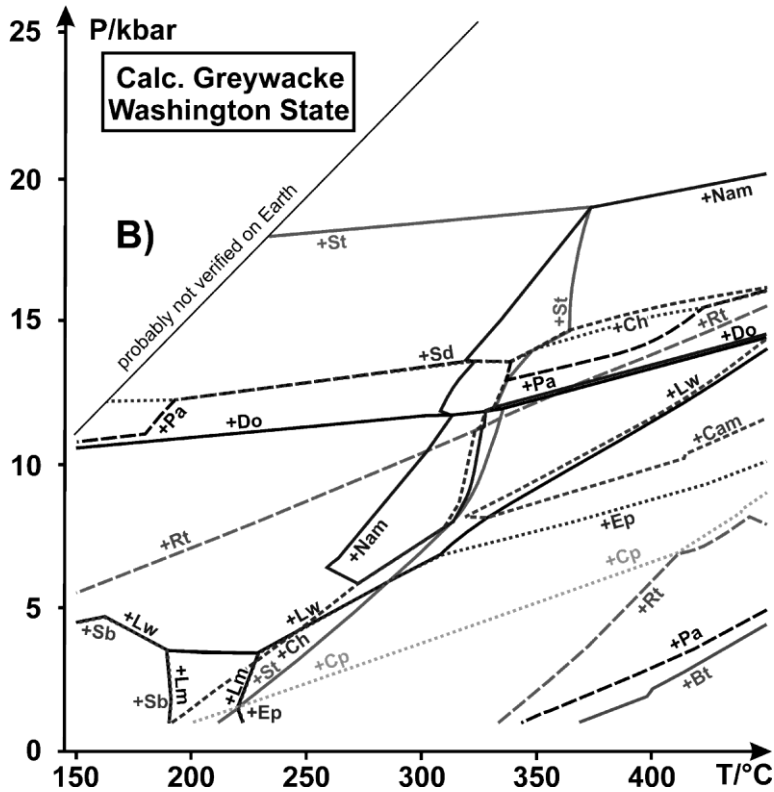


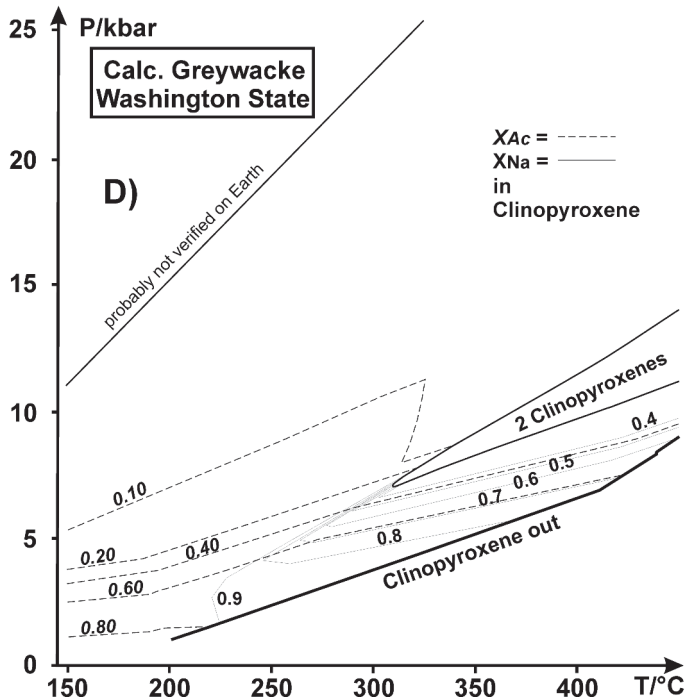
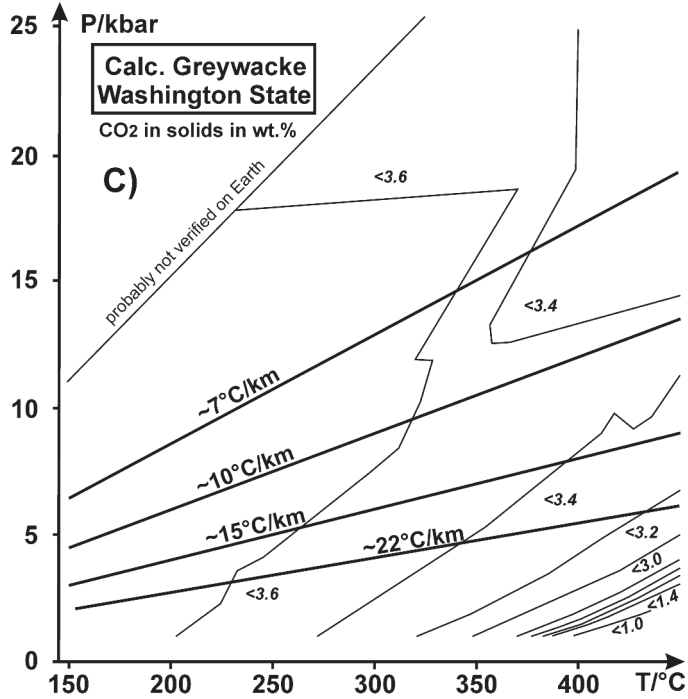
Fig. 1 - a) P-t pseudosection computed for the calcareous greywacke from Washington state the bulk rock composition of which is given in Table 1. Different grey tones of P-t fields refer to different variance of the corresponding mineral assemblage (the darker the higher). a few very small P-t fields are not assigned to a mineral assemblage. b) outlined P-t occurrences of selected phases. c) isopleths related to the CO<sub>2</sub> content in solids given in wt.%. note that the spacing between the isopleths is 0.4 for the range 1.0 to 3.0. specific geotherms are also shown which relate to those mentioned in the text. D) isopleths for molar contents of acmite component and na in clinopyroxene. according to this graph omphacite and jadeite-rich clinopyroxene coexist in a small P-t field. For simplification this field was not shown in the P-t pseudosection of Fig. 1a but mineral assemblages with one clinopyroxene only.

abbreviations for mineral phases are: an = analcime, ar = aragonite, bt = biotite, cam = ca-amphibole, cc = calcite, ch = chlorite, cp = clinopyroxene, Do = dolomite, ep = clinozoisite-epidote, Hm = hematite, Kf = K-feldspar, Lm = Laumontite, Lw = lawsonite, mt = magnetite, nam = na-amphibole, Pa = paragonite, Ph = muscovite-phengite, Pl = plagioclase, rh = rhodonite-rich calcite-rhodonite solid-solution phase, rt = rutile, sb = stilbite, sd = siderite, st = stilpnomelane, tt = titanite.

between garnet and stilpnomelane. Unfortunately, the resulting data show a strong scatter of values for  $K_D = (mn^{2+}/Fe^{2+})$  in garnet /  $(mn^{2+}/Fe^{2+})$  in stilpnomelane. Thus, the  $\Delta G_f$  at standard state of  $mn^{2+}$ -stilpnomelane could only be roughly approximated. a value of -97200 kJ/mol is proposed leading, for example to  $K_D$  values close

to 12 for ca-poor garnet (< 10 mol% grossular) and mg-poor stilpnomelane (< 20 mol% mg-stilpnomelane) at 400°C (20 kbar) compatible with natural occurrences.

For carpholite and sudoite the original expressions in the file newest\_format\_solut.dat had to be re-written in the same style as, for



instance, for chloritoid [model ctd(HP)] - see above) to guarantee their functioning in subprogram vertex.

#### Carbonates

For solid solutions among the four isotopic carbonate end-members calcite, magnesite, siderite, and rhodochrosite, a common non-ideal solid-solution model was created as no corresponding model existed in the used data file newest\_format\_solut.dat. This new model is based on the thermodynamic properties of the four end-members and the use of 4 kJ/mol for the margules parameter describing the symmetric non-ideal solid-solution between magnesite and siderite (Holland and Powell, 1998). For the binary solid-solutions magnesite-calcite and siderite-calcite, known solvus relations were considered to estimate corresponding margules parameters. according to experimentally explored phase relations in the system  $\text{CaCO}_3\text{-MgCO}_3$  (e.g. Irving and Wyllie, 1975) a hypothetical magnesite-calcite solvus can be approximated by a margules parameter of 35 kJ/mol. For the calcite(1)-siderite(2) solvus of Davidson (1994) an asymmetric approach was chosen resulting in two margules parameters  $W_{112}$  and  $W_{122}$  of 13.5 kJ/mol and 21 kJ/mol, respectively. margules parameters for the (symmetric) binary solid-solutions of rhodochrosite with calcite, siderite, and magnesite were estimated on the basis of margules parameters known for corresponding solid solutions of  $\text{Mn}^{2+}\text{-Ca-Fe}^{2+}\text{-Mg}$  in silicates as in garnet. the resulting estimates were 0 kJ/mol for rhodochrosite-calcite, 4 kJ/mol for rhodochrosite-siderite, and 20 kJ/mol for rhodochrosite-magnesite. no ternary margules parameter was introduced.

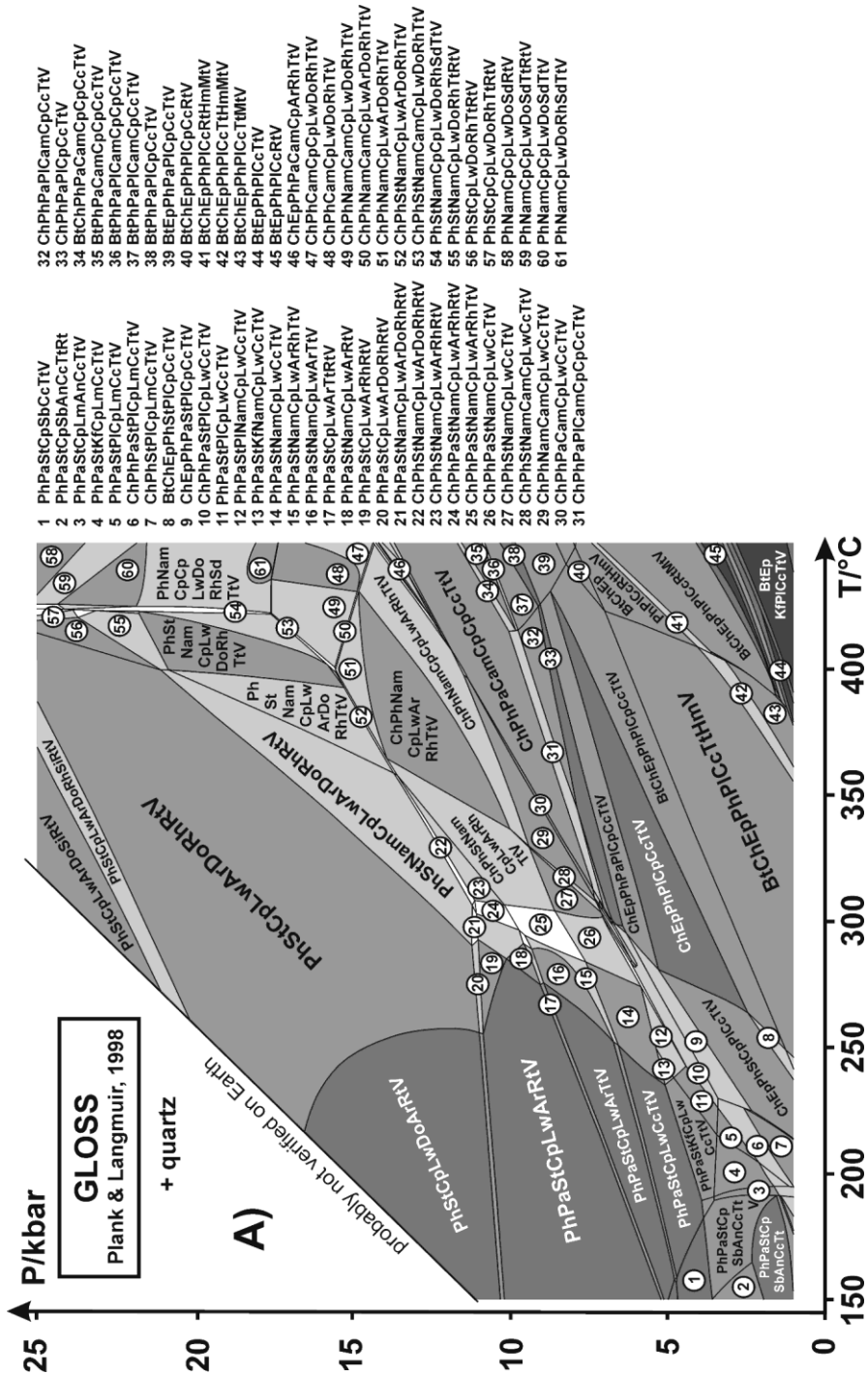
the new model for the quaternary solid-solution in carbonate was subdivided in order to distinguish calcite-rhodonite (model 'mscr1') from magnesite-siderite (model 'mscr2') in the P-t pseudosections produced with *PerPLe\_X*.

For this reason the following limits were set after testing:  $X_{\text{Mg}} \leq 0.1$ ,  $X_{\text{Fe}} \leq 0.5$  for mscr1 and  $X_{\text{Ca}} \leq 0.1$ ,  $X_{\text{Fe}} \geq 0.3$  for mscr2. For dolomite, the model for the binary dolomite-ankerite solid-solution by Holland and Powell (1998) was taken. However, this model in file newest\_format\_solut.dat had to be re-written as in the case of the sudoite model mentioned above. aragonite was considered to be a pure phase.

#### CaLcULation results

##### Phase relations

the P-t pseudosections obtained for the two compositions with relatively low  $\text{CO}_2$  contents (see Table 1) are shown in Figures 1 and 2 for the P-t range of 1-25 kbar and 150-450°C. these figures also display the P-t ranges of critical minerals related to the used whole-rock compositions. the following characteristics are discernable: (1) Quartz is present at all P-t conditions of the pseudosections. (2) muscovite-phengite occurs at almost all P-t conditions except at the highest temperatures and lowest pressures considered (Fig. 3) where K-feldspar appears instead. the si contents of potassic white mica significantly rise with pressure (Fig. 3) similar to those in phengite of the  $\text{CO}_2$ -free metapsammopelite investigated by Massonne and Willner (2008). (3) a second potassium-bearing phase frequently coexists with phengite (or K-feldspar) especially in the P-t pseudosection for the GLoss composition (Fig. 2) which is richer in  $\text{K}_2\text{O}$  than that of the calcareous greywacke from Washington state. conditions for two coexisting K-bearing phases are either relatively low temperatures and high pressures (stilpnomelane-phengite) or high temperatures and low pressures (biotite-phengite/K-feldspar). (4) sodic phases in the P-t pseudosections (see Figs. 1 and 2) are analcime (at the lowest P-t conditions = zeolite facies), paragonite (at intermediate pressures),



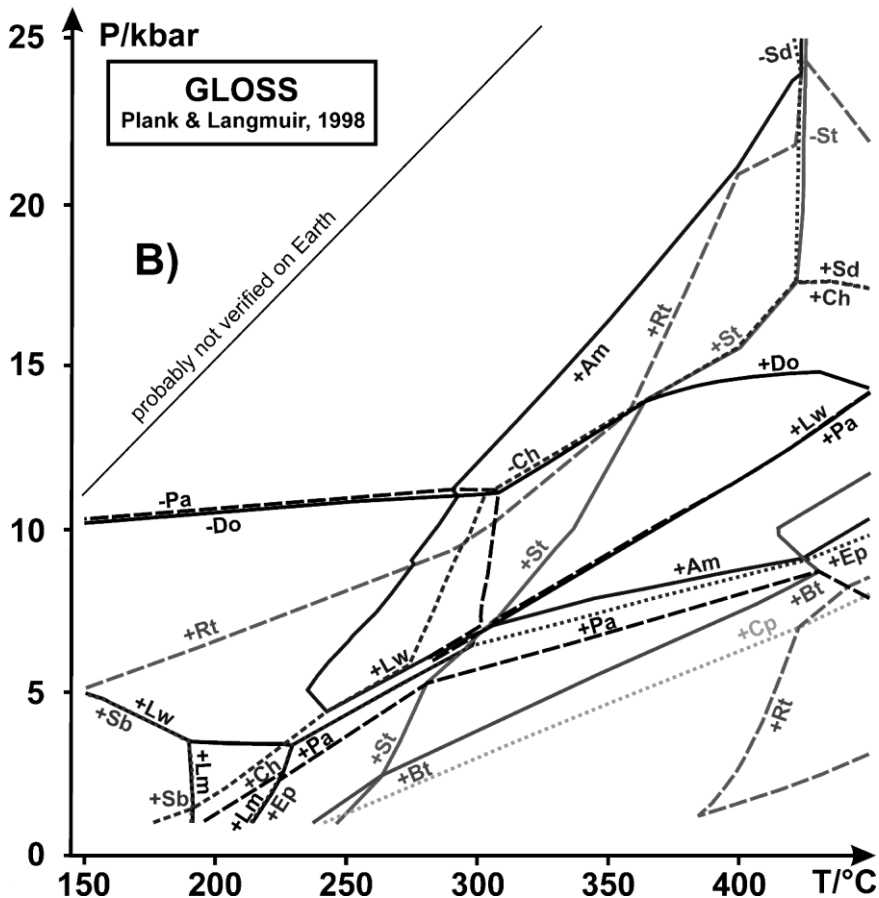


Fig. 2 - a) P-t pseudosection computed for GLOSS (= global subducted sediment) the bulk rock composition of which is given in Table 1. Different grey tones of P-t fields refer to different variance of the corresponding mineral assemblage (the darker the higher). a few very small P-t fields are not assigned to a mineral assemblage. Double cp in a mineral assemblage points to two coexisting clinopyroxenes very similar to the situation shown in Fig. 1D. b) outlined P-t occurrences of selected phases. abbreviations for mineral phases as given in Fig. 1 and am = amphibole, v = H<sub>2</sub>O-rich fluid.

plagioclase (at low pressures and relatively high temperatures - mostly albite but also oligoclase, at  $t > 300^{\circ}\text{C}$  (greywacke) or  $330^{\circ}\text{C}$  (GLOSS), and andesine; the latter only in the greywacke at the highest temperatures and lowest pressures), na-amphibole, and na-rich clinopyroxene. The latter phase is very rich in aegirine component ( $\geq 80\text{ mol}\%$ ) only at the lowest temperatures and pressures (see Fig. 1D). With rising pressure, the content of jadeite significantly increases. For instance at  $300^{\circ}\text{C}$  and 12 kbar, clinopyroxene

contains somewhat less than 10 mol% aegirine component in the calcareous greywacke (Fig. 1D) but still 24 mol% aegirine component in the GLOSS composition because this composition is more highly oxidised compared to the calcareous greywacke. at this P-t condition, clinopyroxene is a jadeite-aegirine solid solution phase without diopside-hedenbergite component. However, along a P-t path from 1 kbar -  $150^{\circ}\text{C}$  to 10 kbar -  $450^{\circ}\text{C}$ , this component can significantly increase (see Fig. 1D). thus, in the

P-t pseudosections for both bulk-rock compositions with relatively low CO<sub>2</sub> contents, a P-t field is present (see Fig. 2a) where jadeite-rich clinopyroxene coexists with a clinopyroxene close to the join diopside-acmite (Fig. 1D) which is, thus, poor in jadeite component. Up to three of the aforementioned sodic phases can coexist, for instance, paragonite + na-amphibole + na-rich clinopyroxene at intermediate P-t conditions. (5) calcic phases in the P-t pseudosections are stilbite and laumontite of the zeolite facies, epidote (at relatively high temperatures and low pressures), lawsonite (at high pressures), and ca-amphibole, which can coexist with na-amphibole in a small P-t area but only in the GLOSS composition (see Fig. 2). moreover, clinopyroxene can contain considerable ca contents as mentioned above. Furthermore, titanite takes the place of rutile at intermediate P-t conditions (see Figs. 1 and 2). (6) in addition to rutile, further oxide phases appear, namely hematite and/or magnetite (the latter only at relatively low pressures). (7) chlorite is the only Fe<sup>2+</sup>-mg silicate phase which occurs in addition to the aforementioned phases stilpnomelane, biotite, and amphibole. Garnet, chloritoid, carpholite and sudoite as well as pumpellyite did not appear in the considered P-t range. the field of chlorite is limited to relatively high temperatures and low to intermediate pressures. (8) carbonate phases are exclusively calcite or aragonite at low to intermediate pressures. Dolomite appears only at high pressures where it can coexist with aragonite (over a significant P-t range only in the P-t pseudosection for GLOSS). a coexistence of dolomite with siderite (over a wide P-t area above 12 kbar only in the P-t pseudosection for the greywacke) and/or relatively mn<sup>2+</sup>-rich carbonate (calcite-rhodochrosite solid-solution) is also notable.

the phase relations calculated for the marly limestone (Fig. 4) show some significant differences from those for the two relatively

CO<sub>2</sub>-poor compositions. these differences are: (1) stilpnomelane is limited to a very small P-t range at very low temperatures. (2) in fact, potassic white mica is an almost omnipresent phase in the P-t pseudosection for the marly limestone but its composition is limited to si contents below 3.20 per formula unit (Fig. 3) even at pressures close to 25 kbar. (3) chlorite occurs already at the lowest temperatures but is limited to pressures of less than 8 kbar only. (4) carpholite is another Fe<sup>2+</sup>-mg silicate phase which appears exclusively in the P-t pseudosection for the marly limestone (around 300°C between 2.5 and 6 kbar) whereas garnet, chloritoid, and sudoite are lacking again. (5) Kaolinite (up to temperatures of almost 300°C), margarite (t > 270°C, P < 10 kbar), diaspore (> 19 kbar), pyrophyllite, and kyanite are also phases which only occur in the P-t pseudosection for the marly limestone, consistent with the relative abundance of al in this rock composition. this might also explain the wide P-t range for paragonite. na-rich clinopyroxene and plagioclase occur only at limited P-t conditions at high pressures and the lowest pressures - highest temperatures, respectively. (6) neither na-amphibole nor ca-amphibole occurs. titanite appears only at the highest temperatures and lowest pressures. (7) Hematite is an almost omnipresent oxide phase. it is only lacking at the highest temperatures - lowest pressures and replaced by goethite at very-low temperatures and high pressures. (8) Dolomite occurs in a wider P-t range (P > 5 kbar). siderite is lacking.

#### Dehydration and decarbonation behaviour

to demonstrate the dehydration behaviour of the studied rocks contoured P-t diagrams were produced showing isopleths for constant contents of water bound to minerals (Fig. 5). similarly, isopleths for contents of carbon dioxide (bound exclusively to carbonates) were constructed and presented for the calcareous

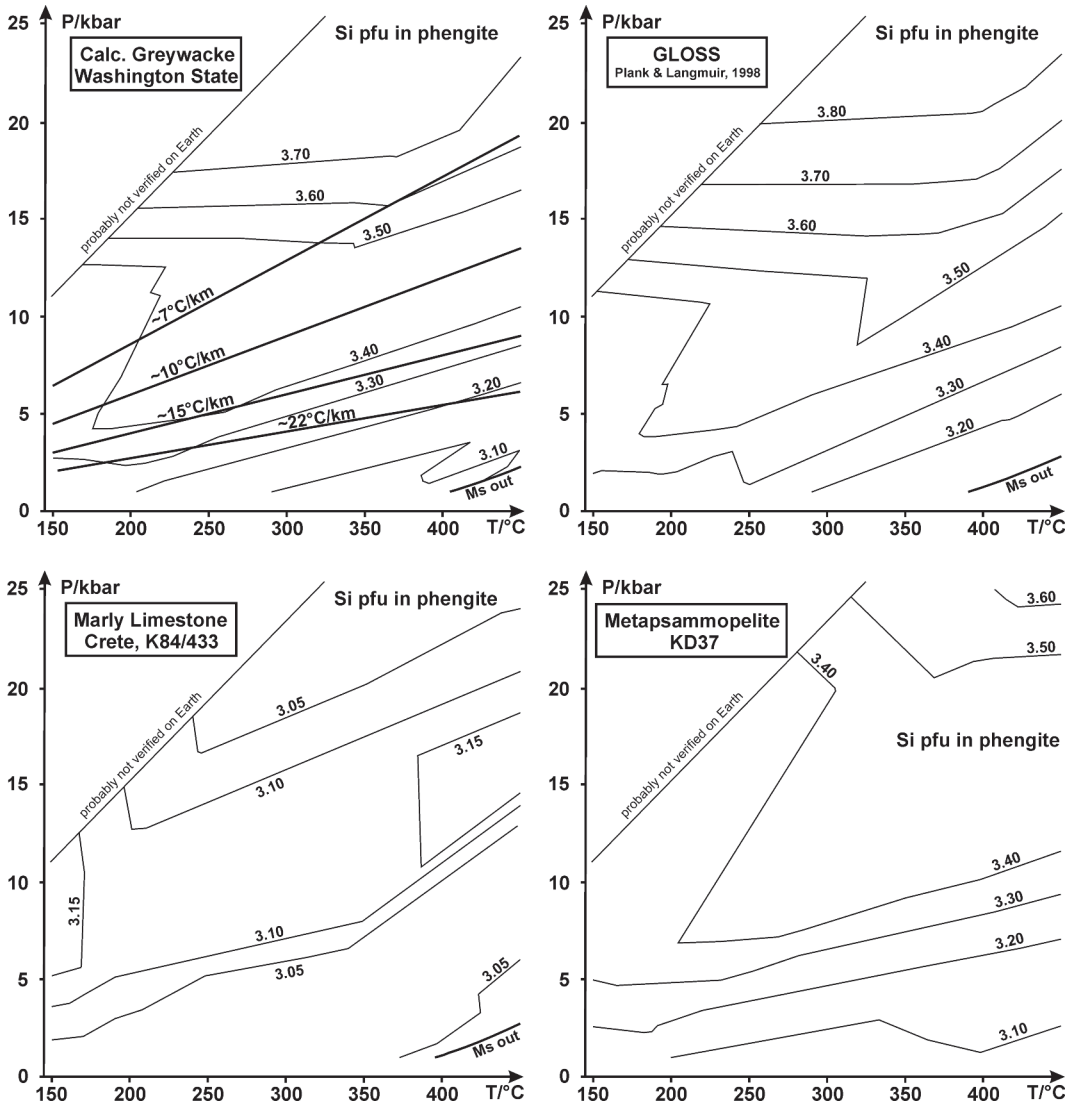
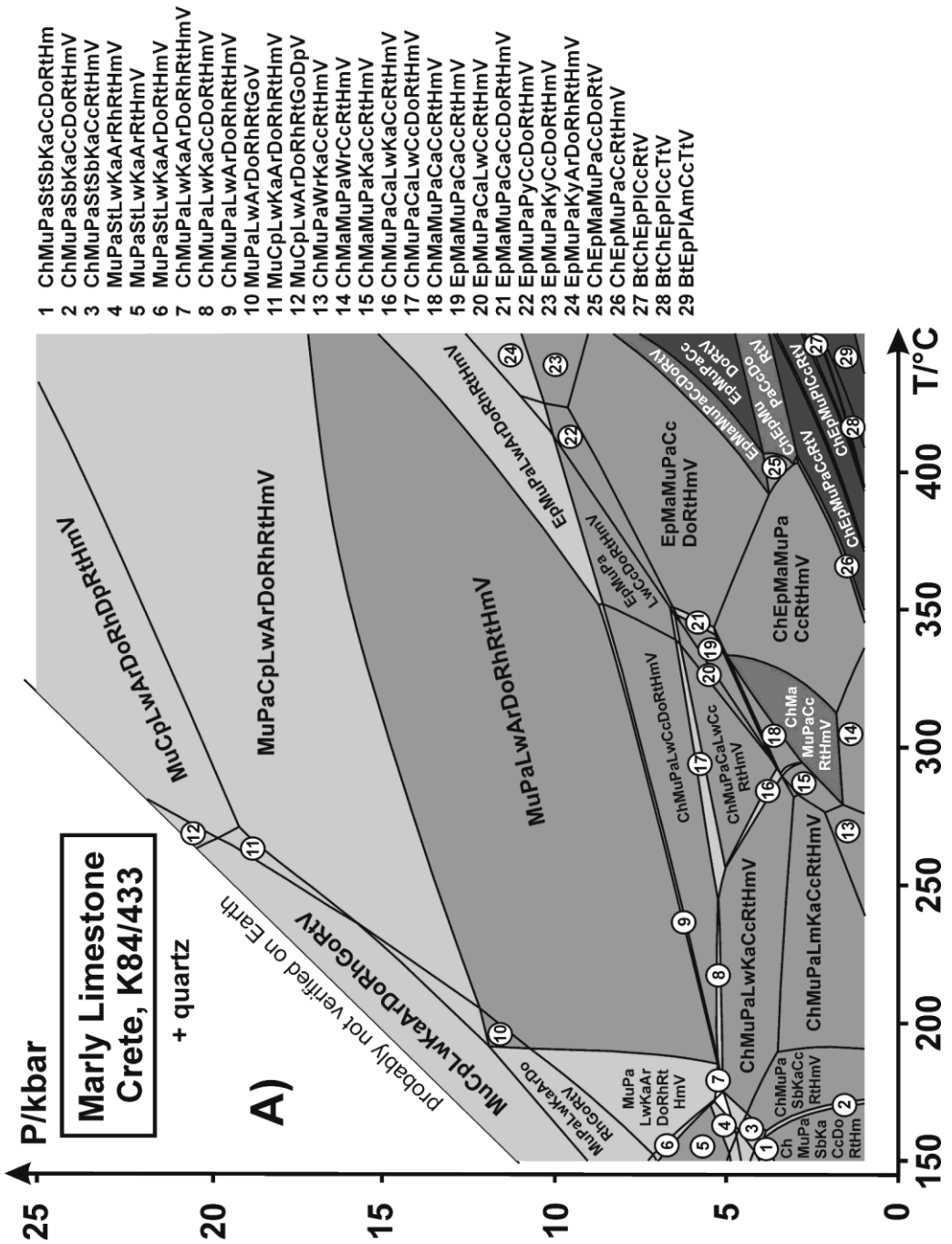


Fig. 3. - si-isopleths for potassic white mica referring to the pseudosections of Figs. 1, 2 and 4 as well as to that given for the metapsammopelite KD37 (for composition see Table 1) by massonne and Willner (2008). "ms out" marks the disappearance of muscovite at low pressures and relatively high temperatures. specific geotherms (see Fig. 1c) are shown in the graph for the calcareous greywacke from Washington state.

greywacke and the marly limestone (Figs. 1 and 4). the tendencies of these isopleths for the GLOSS composition are virtually the same as for

the calcareous greywacke.

according to the H<sub>2</sub>O-isopleths of Fig. 5, the two relatively carbonate-poor metasediments



- 1 ChMuPaSbKaCcDoRtHm
- 2 ChMuPaSbKaCcDoRtHmV
- 3 ChMuPaSbKaCcRtHmV
- 4 MuPaStLwKaArRtHmV
- 5 MuPaStLwKaArRtHm
- 6 MuPaStLwKaArDoRtHmV
- 7 ChMuPaLwKaArDoRtHmV
- 8 ChMuPaLwKaCcDoRtHmV
- 9 ChMuPaLwArDoRtHmV
- 10 MuPaLwArDoRtGoV
- 11 MuCpLwKaArDoRtHmV
- 12 MuCpLwArDoRtGoDpV
- 13 ChMuPaWrKaCcRtHmV
- 14 ChMaMuPaWrCcRtHmV
- 15 ChMaMuPaKaCcRtHmV
- 16 ChMuPaCaLwKaCcRtHmV
- 17 ChMuPaCaLwCcDoRtHmV
- 18 ChMaMuPaCaCcRtHmV
- 19 EpMaMuPaCaCcRtHmV
- 20 EpMuPaCaLwCcRtHmV
- 21 EpMaMuPaCaCcDoRtHmV
- 22 EpMuPaPyCcDoRtHmV
- 23 EpMuPaKyCcDoRtHmV
- 24 EpMuPaKyArDoRtHmV
- 25 ChEpMaMuPaCcDoRtV
- 26 ChEpMuPaCcRtHmV
- 27 BtChEpPICcRtV
- 28 BtChEpPICcTtV
- 29 BtEpPIAmCcTtV

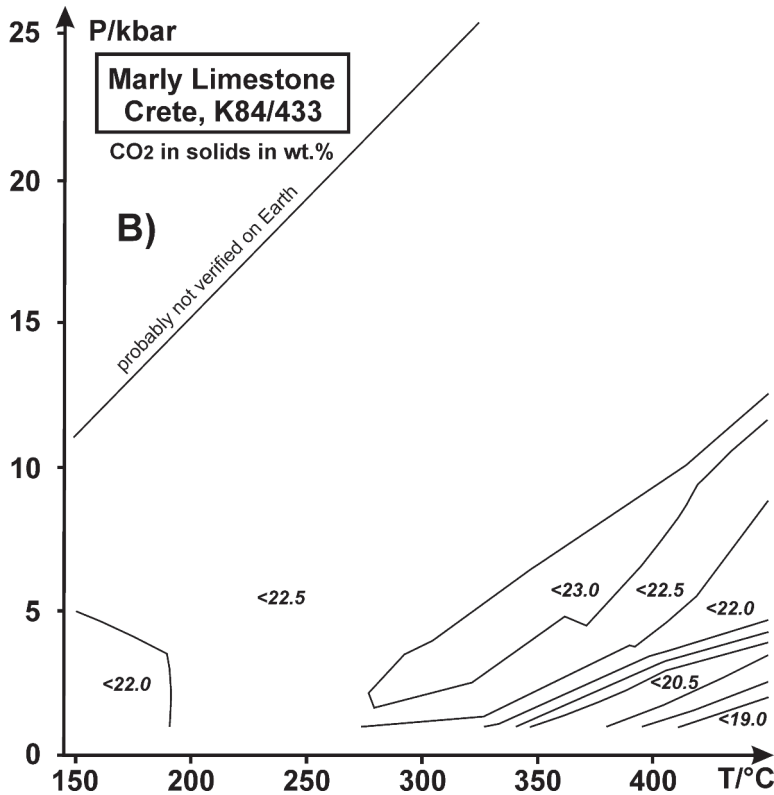


Fig. 4 - a) P-t pseudosection computed for a marly limestone from Crete the bulk rock composition of which is given in Table 1. Different grey tones of P-t fields refer to different variance of the corresponding mineral assemblage (the darker the higher). a few very small P-t fields are not assigned to a mineral assemblage. abbreviations for mineral phases as given in Fig. 1 and: Dp = diasporite, Go = goethite, Ka = kaolinite, Ky = Kyanite, ma = margarite, Py = pyrophyllite, Wr = wairakite, v = H<sub>2</sub>O-rich fluid. b) isopleths related to the CO<sub>2</sub> content in solids given in wt.%.

show very similar dehydration behaviour below 10 kbar and 320°C and this resembles that of the metapsammopelites studied by Massonne and Willner (2008). The cause of the strong dehydration in this P-t range is mainly the breakdown of H<sub>2</sub>O-rich silicates, which are various zeolites, stilpnomelane, and lawsonite. Along geotherms of 15°C/km and higher, fully-hydrated metapsammopelites, including calcareous ones, release about 2.5 (KD37 of Massonne and Willner, 2008) to 4.5 (Gloss) wt.% H<sub>2</sub>O over a temperature interval of 100°C

or less starting between 160 to 180°C. In fact, along geotherms typical for subducted oceanic crust of 7°C/km or less, such rocks are also subjected to a dehydration event (zeolite decomposition at t < 180°C), but only 1-2 wt.% H<sub>2</sub>O is released (Fig. 5). Furthermore, no significant dehydration would occur in the (calcareous) metapsammopelites during deeper subduction until temperatures of 320°C (see KD37) and more (see Gloss) or pressures around 20 kbar are reached. The latter limit, which is discernable only for the psammopelitic

composition KD37, is due to the (partial) decomposition of the H<sub>2</sub>O-rich mineral carpholite (see massonne and Willner, 2008). nevertheless, for geotherms less than 6°C/km, more than 4 wt.% H<sub>2</sub>O (KD37, GLoss) or at least close to 3 wt.% H<sub>2</sub>O (in minerals) can be transported in subduction zones to depths of 80 km (~25 kbar) and more (see Li *et al.*, 2008). For intermediate geotherms (8-15°C/km), for instance, those labelled 'basal accretion' in Fig. 5, a dehydration event after zeolite breakdown occurs at temperatures between 250-450°C, strongly dependent on the exact geothermal gradient. Partly, this event, which releases ca. 1 wt.% H<sub>2</sub>O, takes place in a narrow temperature interval (see especially KD37: ~15°C). However, this event can also be smeared over a wider temperature interval.

a considerable decomposition of carbonates is not found for the studied compositions except at the highest temperatures and lowest pressures addressed here (Figs. 1 and 4). considering geotherms lower than 22°C/km and  $t < 400^\circ\text{C}$ , the resulting X(CO<sub>2</sub>) of the fluid phase for GLoss and the calcareous greywacke is generally below 0.02. along geotherms below 14°C/km this value is  $\leq 0.01$  at the studied temperatures. For the marly limestone, the calculated X(CO<sub>2</sub>) of the fluid phase is consistently higher than for the two other studied rock compositions at the same P-t conditions, but still below 0.08 and 0.03 for geotherms below 15°C/km and 10°C/km, respectively. at 450°C and 1 kbar a X(CO<sub>2</sub>) value for the fluid phase of 0.28 was calculated for the composition of the marly limestone (0.135 for GLoss, 0.19 for the greywacke). However at P-t conditions of  $\geq 7$  kbar and  $\leq 350^\circ\text{C}$ , these values are below 0.01. as a result of this behaviour of the fluid phase, the content of CO<sub>2</sub> in solids is virtually constant (Fig. 1c) or can even increase a bit with rising temperatures (Fig. 4b) except at higher geotherms, because at (very) low temperatures carbonates virtually cannot be decomposed

along low geotherms but hydrous minerals are, leading to a reduction of the mass of solids.

#### Discussion and conclusions

Reliability of the calculated phase relations

the reliability of the applied calculation method was already addressed for metasediments at medium- to high-grade metamorphic conditions by numerous earlier works (e.g., Powell and Holland, 1990) resulting in a general acceptance of the corresponding calculation results. the construction of P-t pseudosections and P-t grids, applying thermodynamic data sets especially that of Holland and Powell (1998), has meanwhile become a standard method for deducing P-t paths, which describe the metamorphic evolution of rocks. However, the quality of corresponding calculation results for the temperature range addressed here could suffer from not well-known thermodynamic data for the relevant solid-solution series. certainly not well-known are the thermodynamic properties of the solid-solution phase stilpnomelane, because, for instance, experimental data are lacking. However, thermodynamic data even for the common solid-solution phases biotite and chlorite, despite considerable experimental efforts relevant to medium metamorphic grade (e.g. massonne and schreyer, 1989; massonne, 1989), are also far off being perfect. For instance, massonne and Willner (2008) noted that the calculated si contents of these phyllosilicates in a psammopelitic composition (300-450°C) are significantly too high (close to 3.0 pfu = per formula unit, as observed here as well) compared to these minerals in corresponding natural rocks. nevertheless, thermodynamic calculations with the same chlorite and biotite solid-solution models (Holland *et al.*, 1998; Powell and Holland, 1999) at medium-grade metamorphic conditions yield reasonable results (see above). another problematic phase might be even potassic white mica although the thermodynamic data are well constrained by

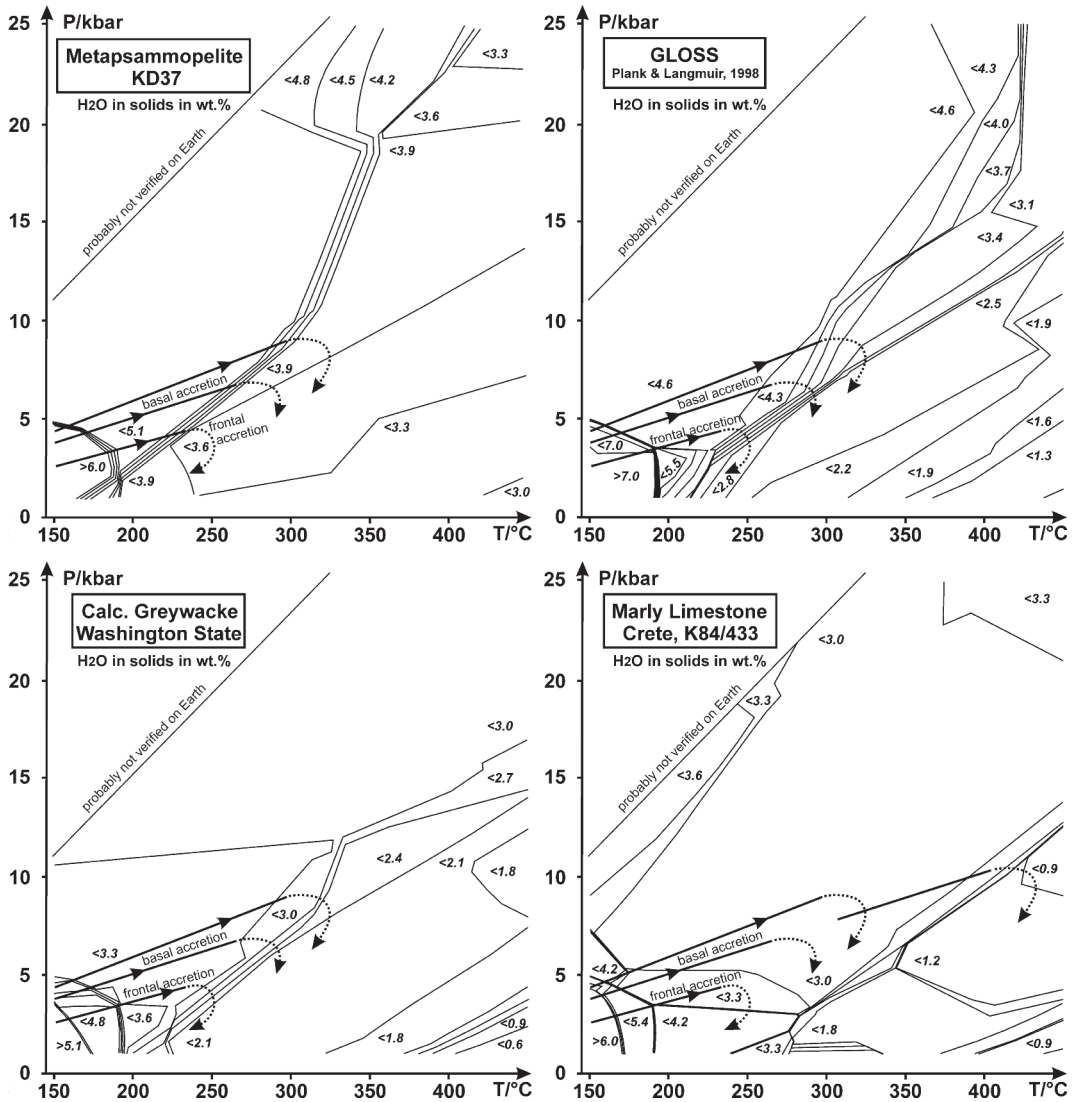


Fig. 5 - isopleths for H<sub>2</sub>O (in wt.%) bound to solids calculated for metapsammopelite KD37 (results were taken from massonne and Willner, 2008), calcareous greywacke from Washington state, GLOSS and a marly limestone from crete (bulk rock compositions are given in Table 1). corresponding phase relations are shown in Figs. 1, 2, and 4. schematic prograde P-T paths (solid = before accretion, dotted = after accretion) are related to two kinds of formation of fossil accretionary wedges in Phanerozoic times as given in massonne and Willner (2008). in case of the marly limestone from crete, the P-T path for basal accretion was extended to temperatures of 400°C and more. such a path might be even realistic for the cretan PQ unit, from which the marly limestone was taken, but it was referred to accretion of a microcontinent (brix *et al.*, 2002). according to the method in constructing such isopleths (cf. connolly, 2005) their precision in terms of P-T position is estimated to be ± 5°C and ± 300 bar.

experimental data (see massonne and szpurka, 1997). First it is worth mentioning that the solid-solution model (Holland and Powell, 1998) applied here considers only four end-member components. minor components considering Ti and Fe<sup>3+</sup> contents in potassic white mica are lacking. The same is true for the trioctahedral-mica component which was experimentally confirmed by massonne and schreyer (1986). in fact, an enlarged potassic white mica model was already introduced by massonne (1992) and successfully applied to low-grade metamorphic rocks (e.g. massonne, 1995; Willner *et al.*, 2009), but such complicated models, introduced into the solid-solution file of `PerPLe_X`, could easily cause an overflow of pseudocomponent compounds or at least a loss of resolution and precision. Furthermore, the problem of a deficit of interlayer cations (ideally 1.0 pfu) exists for low grade metamorphic rocks. This deficit could be assigned to a pyrophyllite component in potassic white mica (e.g. Parra *et al.*, 2002). agard *et al.* (2001) have demonstrated that it is possible to drastically change the dP/dT-slope of Si isopleths for this mica, as displayed in Fig. 3, at low temperatures by the consideration of a significant increase of the pyrophyllite component from 400°C (0% pyrophyllite component) to 250°C (>40% pyrophyllite component). Unfortunately, it is not clear if this pyrophyllite component really exists in very-low to low grade potassic white-mica because the deficit in interlayer cations could also be explained by alkali loss under the electron beam of the electron microprobe, usually applied to analyze potassic white-mica, or a late-stage alteration by the substitution:  $K^+ + Fe^{2+} = \square + Fe^{3+}$ . Hints at such mechanism are medium-grade potassic white-micas which can also show an interlayer-site occupancy lower than 1.0 pfu. in addition, it is not clear yet if H<sub>2</sub>O molecules or H<sub>3</sub>O<sup>+</sup> cations are introduced instead of alkali cations at very-low to low-grade conditions.

in spite of the imperfectness of the used thermodynamic data exemplary outlined above,

the phase relations calculated here and by massonne and Willner (2008) for metapelites and metabasites down to 150°C do not seem to be in conflict with previously derived phase relations (e.g. Frey *et al.*, 1991) for very-low to low grades of metamorphism. in addition, the derivation of P-T conditions for natural rocks (metamorphic temperatures around 300°C) with the thermodynamic data used here leads to reasonable results (Willner *et al.*, 2009). Thus, it can be assumed that the deduced dehydration behaviour at prograde metamorphism (Fig. 5), using the here applied method, should match the right tendencies for the modelled bulk compositions.

#### Application to accretionary wedges and subduction zones

Under the provision that clastic sedimentary material on top of a subducting slab is broadly hydrated at temperatures below 150°C, massonne and Willner (2008) concluded from the results of their calculations that prograde metamorphism of this material along different geotherms in the very-low to low-grade range results in distinct dehydration characteristics: (1) if a cold subduction (geotherms ≤ 8°C/km) is realized no (significant) dehydration takes place after exiting the stability range of relevant zeolites (< 5 kbar, < 150°C) until mantle depths (≥ 20 kbar) are reached. Hence, no clastic sedimentary material is accreted (see also below) along active continental margins and, thus, metapsammopelites are carried into the mantle as it is assumed to be realized in subduction channels of young oceanic-continental collision zones. (2) subduction at hotter conditions (geotherms of 9-12°C/km - see Fig. 5) can lead to basal accretion. These geodynamic processes can, in fact, bring metapelites to relatively great depth but the dehydration of metapsammopelites at 270-300°C and depths ≥ 25 km stops further subduction of this clastic sedimentary material. (3) earlier (or beginning of) subduction (after

passive margin conditions) at still hotter conditions (geotherms of 13-15°C/km), associated with frontal accretion, results in dehydration of psammopelitic material in two steps. a first dehydration step at temperatures somewhat above 150°C (for basal accretion at lower  $t$ ) is due to the breakdown of zeolite (stilbite). a more pronounced second step occurs mainly by breakdown of stilpnomelane at temperatures between 210 and 240°C, i.e. still within the field of brittle deformation. this dehydration event, as well as that at somewhat higher temperatures during basal accretion, softens the rocks so that metapsammopelites are scraped off the subducting oceanic slab at still relatively shallow depths to form accretionary wedge complexes.

For the cold subduction, the conclusion by massonne and Willner (2008) can broadly hold true also for the three here newly studied rock compositions although some differences can be noted for the dehydration behaviour among these rocks (Fig. 5). For instance in case of the marly limestone (Figs. 4 and 5), the breakdown of goethite and kaolinite (minerals which appear due to the relatively oxidised and al-rich rock composition) leads to release of some water at very low geotherms ( $\leq 4^\circ\text{C}/\text{km}$ ) and high pressures (15-20 kbar). in case of the metapsammopelite KD37 at  $P > 19$  kbar and low geotherms, some water is also released due to the breakdown of carpholite (formation of chloritoid) which is lacking in rocks with compositions of the calcareous greywacke and GLOSS because they are significantly poorer in al (see Table 1). For the GLOSS composition a significant dehydration event around 400°C ( $P > 15$  kbar) mainly results from the breakdown of stilpnomelane. this event does not take place in the calcareous greywacke although its composition is similar to that of the GLOSS. in spite of the differences outlined above, the content of water stored in minerals at 450°C and 25 kbar is fairly similar (close to 3 wt.%; about

half of the original water content at near-surface conditions) for all studied compositions (KD37 included), perhaps a surprise because the marly limestone contains high quantities of carbonate minerals. these minerals show hardly any decomposition to release  $\text{CO}_2$  during cold subduction (see also Kerrick and Connolly, 2001).

along higher geotherms (9-15°C/km, see the P- $t$  paths related in Fig. 5 to accretionary processes in Phanerozoic times), carbonate minerals also show hardly any decomposition but again various dehydration reactions proceed. especially, dehydration above 270°C is very conspicuous along the P- $t$  paths assigned to basal accretion for all studied carbonate-poor compositions. compared to the carbonate-free composition KD37, this dehydration event occurs at only somewhat higher temperatures (up to 30°C) in both calcareous greywacke and GLOSS. this is also true for P- $t$  paths related to frontal accretion (see Fig. 5). thus, the above conclusion in regard of the softening of metapsammopelites and their detachment from a subducting oceanic slab (massonne and Willner, 2008) is applicable to carbonaceous greywackes as well. but can a pile of carbonate-rich clastic sediments also be involved in such a dehydration-controlled process? in fact, a similar dehydration event occurred in the marly limestone from crete but at significantly higher temperatures. a possible P- $t$  path for basal accretion, extended to temperatures above 350°C, would crosscut the  $\text{H}_2\text{O}$  isopleths for the marly limestone at temperatures around 400°C (Fig. 5). the corresponding pressures are around 10 kbar, which are related to 40 km earth's depth. this could already be too deep for generating or contributing to an accretionary wedge system (see, e.g., ring *et al.*, 1999). Under these circumstances, it is of interest to consider the geodynamic situation of crete (in oligocene to miocene times - see Jolivet *et al.*, 1996), where the studied marly limestone was

sampled from the PQ unit. This unit in western Crete had experienced peak P-t conditions of 10 kbar at 400 to 450°C (Brix *et al.*, 2002). These conditions, indeed, coincide very well with those at which major dehydration in the marly limestone occurs (Fig. 5), mainly due to breakdown of lawsonite (Fig. 4). In fact, the exhumation of the PQ unit (and also adjacent units) is explained by an oblique buoyant escape within a few million years (Brix *et al.*, 2002) after a preceding collision of a microcontinent (Crete), which was subducted and accreted along the European continental margin, but dehydration could also have triggered this detachment and, thus, the subsequent exhumation event.

#### General conclusions

Although only a few metapsammopelites have been studied here and in a previous work (Massonne and Willner, 2008), it is obvious that somewhat different phase relations in corresponding P-t pseudosections for very-low to low grades of metamorphism (compare, e.g., Figs. 1 and 2) result despite similar rock compositions. Nevertheless, the dehydration behaviour of such rocks can be fairly similar. There are several main stages for the release of H<sub>2</sub>O in prograde metamorphism: (1) For all geotherms, such a stage is related to the crossing of the boundaries of the zeolite fields at temperatures of 150-200°C (or at even lower temperatures at very low geotherms). (2) For very low geotherms ( $\leq 6^\circ\text{C}/\text{km}$ ), an additional dehydration stage is also discernible (only for KD37 and GLoss, see Fig. 5) at pressures above 15 kbar and temperatures between 320°C (or even lower at extremely low geotherms) and 420°C. (3) For geotherms typical for a basal accretion process (around  $10.5^\circ\text{C}/\text{km}$ ), a second major dehydration stage occurs in the temperature range 270 to 320°C. (4) For geotherms higher than  $15^\circ\text{C}/\text{km}$ , this second

stage can in part be smeared over a wider temperature range (see GLoss of Fig. 5) and start already at 200°C. As a result of these dehydration events, the content of water bound to minerals at 450°C is about 50% and 25-35% of the original content (close to surface conditions) for a very low geotherm and a higher geotherm (e.g.  $25^\circ\text{C}/\text{km}$ ), respectively.

The marly limestone shows a dehydration behaviour that is relatively similar to those of the metapsammopelites although the aforementioned second major dehydration event occurs almost 100°C higher (at a fixed pressure) compared to these rocks. For temperatures below 450°C and low geotherms relevant to subduction and accretion processes, the mixed H<sub>2</sub>O-CO<sub>2</sub> fluid contains hardly any CO<sub>2</sub> even when coexisting with the marly limestone. This fact was also stressed by Kerrick and Connolly (2001) for higher temperatures in a subduction zone.

Dehydration events at very-low to low-grade metamorphic conditions can be correlated with specific geodynamic processes requiring a particular rheological behaviour of rocks, which in turn is controlled by the availability of free water in these rocks. For instance, such a correlation was reported by Massonne and Willner (2008) in regard of accretionary wedge systems. The evolution of such systems starts just after passive margin conditions and, thus, with geotherms, which are relatively high compared to those typical for evolved subduction settings. These geotherms, affecting the sedimentary pile on top of subducting oceanic crust, decrease during continuous subduction and the build-up of the accretionary wedge system (e.g. Gerya *et al.*, 2002). For instance, when corresponding geotherms between 10 and  $12^\circ\text{C}/\text{km}$  are reached, major dehydration of clastic sediments with or without some carbonate occurs at temperatures around 300°C, leading to the detachment of these sediments at depths of 20-35 km (basal accretion), whereas the basic underlayer does not

dehydrate at this stage (massonne and Willner, 2008) and is, thus, transported further downwards. carbonate-rich sediments, however, might behave differently. These rocks are either transported to mantle depths, as clastic sediments would if cold subduction with geotherms below 8°C/km are realized (massonne and Willner, 2008), or accreted at greater depths than the clastic sediments. The above discussed example of the low-temperature, high-pressure PQ unit of Crete confirms the possibility of such an accretion process at greater depths. In ancient times with generally higher geotherms in subduction zones, no such accretion especially of carbonate-rich sediments would have occurred. On the contrary, decarbonation of the top of the oceanic crust subducted in Archean times, as proposed by Santosh and Omori (2008), could have proceeded (see CO<sub>2</sub> isopleths of Fig. 4), although it is questionable if a corresponding process would be a true subduction or rather an underthrust event.

#### Acknowledgments

The manuscript benefitted from critical reviews by B.W. Evans and D. Castelli; the latter also revised the Italian abstract.

#### References

- AGARD P., VIDAL O. and GOFFÉ B. (2001) - *Interlayer and Si content of phengite in HP-LT carpholite-bearing metapelites*. *J. metam. Geol.*, **19**, 479-495.
- BERMAN R.G. and BROWN T.H. (1985) - *Heat capacity in the system Na<sub>2</sub>O-K<sub>2</sub>O-CaO-MgO-FeO-Fe<sub>2</sub>O<sub>3</sub>-Al<sub>2</sub>O<sub>3</sub>-SiO<sub>2</sub>-TiO<sub>2</sub>-H<sub>2</sub>O-CO<sub>2</sub>: representation, estimation, and high temperature extrapolation*. *contrib. mineral. Petrol.*, **89**, 168-183.
- BRIX M.F., STÖCKHERT B., SEIDEL E., THEYE T., THOMSON S.N. and KÜSTER M. (2002) - *Thermobarometric data from a fossil zircon partial annealing zone in high pressure - low temperature rocks of eastern and central Crete, Greece*. *tectonophys.*, **349**, 309-326.
- BROWN E.H. (1975) - *A petrogenetic grid for reactions producing biotite and other Al-Fe-Mg-silicates in the greenschist facies*. *J. Petrol.*, **16**, 258-271.
- CHATTERJEE N.D. and FROESE E. (1975) - *A thermodynamic study of the pseudobinary join muscovite-paragonite in the system KAlSi<sub>3</sub>O<sub>8</sub>-NaAlSi<sub>3</sub>O<sub>8</sub>-Al<sub>2</sub>O<sub>3</sub>-SiO<sub>2</sub>-H<sub>2</sub>O*. *am. mineral.*, **60**, 985-993.
- CONNOLLY J.A.D. (2005) - *Computation of phase equilibria by linear programming: A tool for geodynamic modeling and its application to subduction zone decarbonation*. *earth Planet. sci. Letters*, **236**, 524-541.
- DAVIDSON P.M. (1994) - *Ternary iron, magnesium, calcium carbonates: A thermodynamic model for dolomite as an ordered derivative of calcite-structure solutions*. *am. mineral.*, **79**, 332-339.
- EVANS B.W. (1990) - *Phase relations of epidote-blueschists*. *Lithos*, **24**, 3-23.
- FRANZ G., HINRICHSSEN T. and WANNEMACHER E. (1977) - *Determination of the miscibility gap on the solid solution series paragonite-margarite by means of the infrared spectroscopy*. *contrib. mineral. Petrol.*, **59**, 307-316.
- FREY M., DE CAPITANI C. and LIOU J.G. (1991) - *A new petrogenetic grid for low-grade metabasites*. *J. metam. Geol.*, **9**, 497-509.
- FUHRMAN M.L. and LINDSLEY D.H. (1988) - *Ternary-feldspar modeling and thermometry*. *am. mineral.*, **73**, 201-215.
- GERYA T.V., STÖCKHERT B. and PERCHUK A.L. (2002) - *Exhumation of high-pressure metamorphic rocks in a subduction channel: a numerical simulation*. *tectonics*, **21**, 6-1 - 6-19.
- GOTO A., KUNUGIZA K. and OMORI S. (2007) - *Evolving fluid composition during prograde metamorphism in subduction zones: A new approach using carbonate-bearing assemblages in the pelitic system*. *Gondwana res.*, **11**, 166-179.
- HOLLAND T.J.B. (1989) - *Dependence of entropy on volume for silicate and oxide minerals: A review and a predictive model*. *am. mineral.*, **74**, 5-13.
- HOLLAND T.J.B. and POWELL R. (1998) - *An internally consistent thermodynamic data set for phases of petrological interest*. *J. metam. Geol.*, **16**, 309-343.
- HOLLAND T.J.B., BAKER J. and POWELL R. (1998) - *Mixing properties and activity-composition relationships of chlorites in the system MgO-FeO-*

- $Al_2O_3$ - $SiO_2$ - $H_2O$ . eur. J. mineral., **10**, 395-406.
- Irvin G. A. J. and Wyllie P. J. (1975) - *Subsolidus and melting relations for calcite, magnesite and the join  $CaCO_3$ - $MgCO_3$  to 36 kb*. Geochim. cosmochim. acta, **39**, 35-53.
- Jolivet L., Goffé B., Monié P., Truffert-Luxey C., Patriat M. and Bonneau M. (1996) - *Miocene detachment in Crete and exhumation P-T-t paths of high-pressure metamorphic rocks*. tectonics, **15**, 1129-1153.
- Kerrick D. M. and Connolly J. A. D. (2001) - *Metamorphic devolatilization of subducted marine sediments and the transport of volatiles into the Earth's mantle*. nature, **411**, 293-296.
- Li Y., Massonne H.-J., Willner A. P., Tang H. and Liu C. (2008) - *Dehydration of clastic sediments in subduction zones: a theoretical study using thermodynamic data of minerals*. island arc, **17**, 577-590.
- Lio J. G., Maruyama S. and Cho M. (1985) - *Phase equilibria and mineral parageneses of metabasites in low-grade metamorphism*. mineral. mag., **49**, 321-333.
- Lio J. G., Maruyama S. and Cho M. (1987) - *Very low-grade metamorphism of volcanic and volcanoclastic rocks - mineral assemblages and mineral facies*. in: "Low temperature metamorphism", M. Frey (ed.), Blackie & Son Ltd., Glasgow, 59-113.
- Massonne H.-J. (1989) - *The upper thermal stability of magnesian chlorite + quartz: an experimental study in the system  $MgO$ - $Al_2O_3$ - $SiO_2$ - $H_2O$* . J. metam. Geol., **7**, 567-581.
- Massonne H.-J. (1992) - *Thermochemical determination of water activities relevant to eclogitic rocks*. in: Water-rock interaction, Proc. 7th int. symp., Park city, Utah, U.S.A., vol. 2, moderate and high temperature environments, Y. K. Kharaka and A. S. Maest (eds.), Balkema, Rotterdam, 1523-1526.
- Massonne H.-J. (1995) - *III. Rhenohercynian Foldbelt, C. Metamorphic units (Northern phyllite zone), 4. Metamorphic evolution*. - in: "Pre-Permian geology of central and eastern Europe", R. D. Dallmeyer, W. Franke and K. Weber (eds.), Springer, Berlin, 132-137.
- Massonne H.-J. and Schreyer W. (1986) - *High-pressure syntheses and X-ray properties of white micas in the system  $K_2O$ - $MgO$ - $Al_2O_3$ - $SiO_2$ - $H_2O$* . n. Jb. miner. abh., **153**, 177-215.
- Massonne H.-J. and Schreyer W. (1989) - *Stability field of the high-pressure assemblage talc + phengite and two new phengite barometers*. eur. J. mineral., **1**, 391-410.
- Massonne H.-J. and Szpürka Z. (1997) - *Thermodynamic properties of white micas on the basis of high-pressure experiments in the systems  $K_2O$ - $MgO$ - $Al_2O_3$ - $SiO_2$ - $H_2O$  and  $K_2O$ - $FeO$ - $Al_2O_3$ - $SiO_2$ - $H_2O$* . Lithos, **41**, 229-250.
- Massonne H.-J., Willner A. P. and Gerya T. (2007) - *Densities of metapelitic rocks at high to ultrahigh pressure conditions: what are the geodynamic consequences?* earth Planet. sci. Letters, **256**, 12-27.
- Massonne H.-J. and Willner A. P. (2008) - *Dehydration behaviour of metapelites and mid-ocean ridge basalt at very-low to low grade metamorphic conditions*. eur. J. mineral., **20**, 867-879.
- Parra T., Vidale R. and Agard P. (2002) - *A thermodynamic model for Fe-Mg dioctahedral K white micas using data from phase-equilibrium experiments and natural pelitic assemblages*. contrib. mineral. Petrol., **143**, 706-732.
- Planck T. and Langmuir C. H. (1998) - *The chemical composition of subducting sediment and its consequences for the crust and mantle*. chem. Geol., **145**, 325-394.
- Pettijohn F. J. (1949) - *Sedimentary rocks*, Harper & Brothers, New York, 526 pp.
- Piber A., Tropper P. and Mirwald P. W. (2009) - *Geothermobarometry of a stilpnomelane-garnet-bearing metapegmatite: P-T constraints on the Eo-Alpine metamorphic overprint of the Austroalpine nappes north of the Tauern Window*. miner. Petrol., **96**, 99-111.
- Powell R. and Holland T. J. B. (1990) - *Calculated mineral equilibria in the pelite system KFMASH ( $K_2O$ - $FeO$ - $MgO$ - $Al_2O_3$ - $SiO_2$ - $H_2O$ )*. am. mineral., **75**, 367-380.
- Powell R. and Holland T. (1999) - *Relating formulations of the thermodynamics of mineral solid solutions: Activity modeling of pyroxenes, amphiboles, and micas*. am. mineral., **84**, 1-14.
- Ting U., Brandon M. T., Willett S. and Lister G. S. (1999) - *Exhumation processes*. in: "Exhumation Processes: normal faulting, ductile flow and

- erosion", U. ring, m.t. brandon, G.s. Lister, s. Willett (eds.), spec. Publ. Geol. soc. London, **154**, 1-27.
- robinson D.J. (1984) - *Silicate facies iron-formation and strata-bound alteration; tuffaceous exhalites derived by mixing; evidence from Mn garnet-stilpnomelane rocks at Redstone, Timmins, Ontario.* econ. Geol., **79**, 1796-1817.
- SantosH m. and Omori s. (2008) - *CO<sub>2</sub> windows from mantle to atmosphere and speculations on the link with melting of snowball Earth.* Gondwana res., **14**, 82-96.
- tHeye t. (1988) - *Aufsteigende Hochdruckmetamorphose in Sedimenten der Phyllit-Quarzit-Einheit Kretas und des Peloponnes.* Diss. Univ. braunschweig, 224 pp.
- tHeye t., SeiDeL e. and viDaL o. (1992) - *Carpholite, sudoite, chloritoid in low-grade high-pressure metapelites from Crete and the Peloponnese, Greece.* eur. J. mineral., **4**, 487-507.
- Willner a.P., Sepúlveda F.a., Hervé F., massonne H.-J. and SUDO m. (2009) - *Conditions and timing of very-low-grade metamorphism in the Early Mesozoic frontal accretionary prism of the Madre de Dios Archipelago (50°20' S; S-Chile).* J. Petrol., **50**, 2127-2155.